Accepted Manuscript

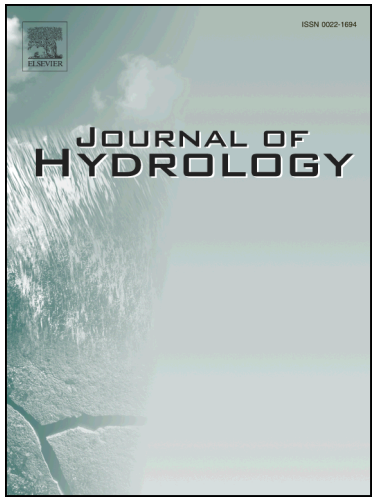

Research papers

Incorporating parameter dependencies into temporal downscaling of extreme rainfall using a random cascade approach

Neil McIntyre, Meng Shi, Christian Onof

PII: S0022-1694(16)30624-2
DOI: http://dx.doi.org/10.1016/j.jhydrol.2016.09.057
Reference: HYDROL 21553

To appear in: *Journal of Hydrology*

Received Date: 22 February 2016
Revised Date: 26 May 2016
Accepted Date: 24 September 2016

Please cite this article as: McIntyre, N., Shi, M., Onof, C., Incorporating parameter dependencies into temporal downscaling of extreme rainfall using a random cascade approach, *Journal of Hydrology* (2016), doi: http://dx.doi.org/10.1016/j.jhydrol.2016.09.057

Incorporating parameter dependencies into temporal downscaling of extreme rainfall using a random cascade approach

Neil McIntyre[a], Meng Shi[a], Christian Onof[b]

a. Sustainable Minerals Institute, The University of Queensland, St Lucia, Brisbane, Queensland, 4072, Australia. n.mcintyre@uq.edu.au*; m.shi@uq.edu.au

b. Department of Civil and Environmental Engineering, Imperial College London, South Kensington, London, SW7 2AZ, UK. c.onof@imperial.ac.uk

*Corresponding author

ABSTRACT

Downscaling site rainfall from daily to sub-daily resolution is often approached using the multiplicative discrete random cascade (MDRC) class of models, with mixed success. Questions in any application – for MDRCs or indeed other classes of downscaling model - is to what extent and in what way are model parameters functions of rainfall event type and/or large scale climate controls. These questions underlie the applicability of downscaling models for analysing rainfall and hydrological extremes, in particular for synthesising long-term historical or future sub-daily extremes conditional on historic or projected daily data. Using fine resolution data from two gauges in central Brisbane, Australia, covering the period 1908-2015, microcanonical MDRC models are fitted using data from 1 day to 11.25 minute resolutions in seven cascade levels, each level dividing the time interval and its rainfall volume into two sub-intervals. Each cascade level involves estimating: the probabilities that all the rainfall observed in a time interval is concentrated in the first and the second of the two sub-intervals; and also two Beta distribution parameters that define the probability of a given division of the rainfall into both sub-intervals. These parameters are found to

vary systematically with time of day, month of year, decade, rainfall volume, event temporal structure and ENSO anomaly. Reasonable downscaling performance is achieved in an evaluation period - in terms of replicating extreme values and autocorrelation structure of 11.25-minute rainfall given the observed daily data - by including the parameter dependence on the rainfall volume and event structure, which involves 16 parameters per cascade level. Using only a volume dependence and assuming symmetrical probability distributions reduces the number of parameters to two per level with only a small loss of performance; and empirical relationships between parameter values and cascade level reduces the total number of parameters to four, with indetectable further loss of performance. Improving the parameterisation of the volume dependence is considered the most promising opportunity for improving at-site performance.

Keywords

Precipitation, downscale, extremes, floods, cascade, Queensland

1 INTRODUCTION

Long-term sub-daily rainfall data are used for many planning and design applications, for example urban drainage, reservoir spillways and levee design, and flood and drought risk management planning. Continuous-time rainfall measurement devices such as tipping bucket gauges provide such data at point scale, often supplemented by a co-located gauge that provides only daily totals. Continuous-time rainfall measurement has been in common use since only the 1970s; furthermore the sub-daily data are often discontinuous and of variable quality due to the challenges of maintaining the equipment and processing the large volumes of data. On the other hand, good quality daily rainfall data often exist more continuously and for longer historical periods, with daily records back to the 19th century not uncommon. Therefore, downscaling available daily records to provide realistic long-term sub-daily data is a relevant and well-studied problem. Advances in high resolution regional climate modelling and remote sensing continue to provide new approaches to downscaling rainfall, especially where the spatial rainfall patterns are important. However, the limited length and accuracy of remote sensing-based rainfall, and challenges of accuracy and computational cost of regional climate models, mean that the reconstruction of long-term sub-daily rainfall still primarily relies on statistical downscaling of daily rain gauge data.

An attractively simple approach to downscaling daily rain gauge data is using multiplicative discrete random cascade (MDRC) models. A MDRC is the procedure of repeatedly dividing a day and its corresponding rainfall volume into smaller discrete time intervals and corresponding volumes until the sought time resolution is reached. For example, a day's rainfall may be divided into two 12-hour rainfall volumes at the first cascade level, which are then both divided into two six-hour volumes in the second cascade level, etc. An example of this is shown in Figure 1. Each interval at each cascade level requires a set of weights W defining how much of the rainfall is allocated to the sub-intervals. For example, R mm of rainfall in one day might be divided into W_1R and W_2R in the first and second 12-hour sub-intervals respectively, where the weights W_1 and W_2 would be sampled from suitable

probability distributions identified from the observed data. An attraction of the MDRC approach is its simplicity - the model development only involves the identification of suitable probability distributions for the W values at each cascade level. Alternative statistical approaches to developing continuous-time sub-daily rainfall series, while having their own strengths, have more complicated model identification procedures (Onof et al. 2000).

FIGURE 1 HERE

Differences between models within the MDRC type primarily relate to the different approaches to estimating the probability distributions for W, and they can be classified into canonical (also called macrocanonical) models and microcanonical models. For canonical models, the probability distribution of weights is typically a log-normal, log-Poisson or log-Levy distribution (Onof et al. 2000, Molnar and Burlando 2005, Sivakumar and Sharma 2008, Lovejoy and Schertzer 2013) with the parameters estimated using a theoretically derived relationship with the scaling properties of the rainfall moments. The weights for adjacent sub-intervals at each cascade level (W_1 and W_2 in the case of dividing into two sub-intervals) are sampled independently from the same distribution so that their sum may be greater than 1.0; in other words the canonical models do not aim to conserve volume when sub-dividing R, except in the trivial case of dividing a zero volume. However, by fixing the mean of the probability distribution (at 0.5 in the case of dividing into two parts), the overall volume balance of the rainfall series is closely preserved.

As opposed to models of the canonical type, microcanonical models preserve volume when sub-dividing rainfall so that in the case of two sub-intervals $W_2=1-W_1$. Also in contrast to the canonical type of model, the probability distributions may be estimated empirically for each cascade level independently, although the same probability distribution is usually assumed across levels. Molnar and Burlando (2005) suggest that a symmetrical Beta distribution is suitable assuming that W_1 and

W_2 are identically distributed (that is, it is equally likely that a given proportion of R falls in the first sub-interval as in the second). Allowing for "intermittency" of rainfall, their model also included the probability that R is transferred into only one of the two sub-intervals, with the Beta distribution applied only to non-intermittency cases. Olsson (1998) used a similar microcanonical approach, although specified a uniform distribution as opposed to the more flexible Beta distribution, and found that the probability of intermittency in any interval was related to whether the surrounding intervals were wet or dry. More in-depth description of a canonical approach is provided by Deidda et al. (1999) and of the microcanonical approach by Olsson (1998), and a summary of both methods is in Molnar and Burlando (2005).

The canonical models have the potential advantage that the theoretical relationships with the moments' scaling properties permit scale invariance of rainfall to be exploited. That is, if the scaling properties of the moments are sufficiently constant over different cascade levels then the probability distribution of weights can be generalised, rather than being identified for each level individually. This has particular advantage where there are no observed data at the sought time-scale and therefore it is not possible to identify a specific probability distribution for that level. Onof et al. (2005) illustrate such an application. Another potential attraction of the canonical approach is its performance in replicating observed statistics of fine scale data - Molnar and Burlando (2005) found that the canonical approach generally performed better in terms of replicating observed variability of 10-minute data from a 20-year record in Zurich, Switzerland; and Pui et al (2009) reached a similar conclusion for hourly data from Sydney. However, Sivakumar and Sharma (2008) warned that the presence of scale invariance and a probability distribution (log-Poisson in their case) that can replicate this scale invariance does not necessarily lead to a successful model in terms of fine scale rainfall statistics.

Microcanonical models have the distinct advantage that they preserve volumes at each interval. While not necessarily being beneficial in terms of the model's ability to replicate extreme value statistics, this is important where credibility of the estimates during particular days or sequences of days is relevant. There is also a potential lack of credibility of the canonical method's lack of upper bound to the downscaled rainfall volume, and it may be speculated that the better performance of the canonical approach in producing high extremes is simply because it is free from volume balance constraints for any interval. Furthermore, the greater empiricism of the microcanonical approach means it is amenable to exploring how distribution functions and their parameter values vary over different time-scales (Licznar at al. 2015); and allowing for intermittency of rainfall seems likely to be important in many applications but is excluded from canonical type analysis.

One question about MDRC models that has not been extensively explored is the potential changes of parameter values over time and how best to incorporate them in the model. It is well known that scaling properties are expected to be related to the weather systems, an obvious example being the scaling differences between frontal and convective type events. It is also well-known that storm events have temporal structure, which means that the division of R into two sub-intervals should not be random but depend on where the interval lies in the temporal evolution of the event. Olsson (1998) illustrated this: Using two years of data from a gauge in Sweden, Olsson showed that probabilities of R being concentrated in the first or second sub-interval or both, termed p(1|0) or p(0|1) or p(x|x), depends on whether the interval in question is preceded or followed by another wet interval. Olsson also demonstrated dependence of these parameters on the interval's rainfall volume, R. Using observed records of between two and five years from six gauges in the UK and Brazil, Guntner et al (2001) confirmed Olsson's result and extended it to show that the probability distribution of non-zero W also depends on R and the wet/dry state of the surrounding intervals. Olsson (1998) and Guntner et al. (2001) also demonstrated the significant seasonal variations in p(1|0), p(0|1) and p(x|x). While there was some weak evidence that the probability distribution of

W varied over different cascade levels, Guntner et al. (2001) elected to use a scale-invariance assumption, recognising the benefits of pooling more data; while Olsson (1998) focused on the levels within which scale invariance could be justified from the data. Rupp et al. (2009) investigated the dependence of parameters on rainfall intensity and found that including the dependence of $p(1|0)$ and $p(0|1)$ in a MDRC model significantly improved performance.

Olsson (1998) and Guntner et al. (2001) illustrate the potential to make the microcanonical MDRC model conditional on season, rainfall volume and the presence of surrounding wet or dry intervals. The potential dependencies of the model on climate oscillations and/or climate change are other factors that may be considered in applications of the microcanonical MDRC approach. These are of practical interest where historic time series of daily rainfall is to be disaggregated based on only a few recent years of fine scale data; and evidence of changes on scaling behaviour may indicate the potential for climate change effects on extreme rainfall. Licznar et al. (2015) provided the first exploration of this by fitting their MDRC model to sub-periods of a 25-year rainfall record. Another area of interest apparently not yet explored is diurnal dependence of the cascade model parameters as noted by Guntner et al. (2001), which is of practical interest where strong regular diurnal patterns exist such as in the case study used in this paper.

This paper develops upon previous works of Olsson (1998), Guntner et al. (2001), Molnar and Burlando (2005), Rupp et al. (2009) and Licznar et al. (2015) on the applicability of microcanonical MDRC models to temporal disaggregation of single site rainfall, and extending these previous works to encompass diurnal and decadal scale variability. The resulting models are evaluated in terms of their ability to synthesise historic fine-scale rainfall from recently observed records. A rainfall data set from Brisbane, Australia from the period 1908-2015 is used. Although representative of only mid-latitude east-coast Australia, the results provide insight into the potential challenges in other regions

with strong diurnal, seasonal, and inter-annual rainfall, and other regions where rainfall is affected by a multitude of large-scale and synoptic-scale climate drivers.

2 DATA AND METHODS

2.1 Rainfall data

The rainfall data, obtained from the Australian Bureau of Meteorology, consist of data from two central Brisbane gauges. The Brisbane Regional Office (27°28'40"S, 153°1'50"E, 38 m above mean sea level) gauge is a pluviograph, which operated from January 1908 until July 1994. A manual rain gauge at the same site recorded daily rainfall since 1840. The new Brisbane gauge, situated approximately 1 km away (27°28'51"S, 153°2'20"E, 8 m above mean sea level) is a tipping bucket gauge that has operated since December 1999. The 6-minute time-series for both gauges are combined for this analysis. Potential non-stationarity due to the change of gauge is included in the data analysis. An 11.25-minute time-series, used for the analysis, was derived by disaggregating each of the original 6-minute volumes into 0.25 minute intervals assuming a uniform distribution over the 6-minute interval and then aggregating to 11.25 minutes, giving the best achievable 11.25-minute aggregation of the original data. An 11.25-minute interval is chosen because it aggregates to one day over 7 cascade levels with two sub-intervals per level, as shown in Figure 1.

The principal gaps in the data are the majorities of the periods 1909-1910, 1994-1999 and 2009-2010. There is no attempt made to fill these or any more minor gaps, and all the analysis done and statistics presented neglect the rainfall that occurred during these gaps. The data were screened to remove data that are noted as doubtful quality in the source files from the Bureau of Meteorology. If any 6-minute value is considered poor quality or is missing then the whole day's data are considered to be missing. The missing data then account for 16 % of the 1908-2015 period. Intervals with 'trace'

rainfall volumes were also omitted from aspects of the analysis, accounting for the large proportion of the intervals, as explained later. A day's data is defined by the time-step beginning 00:00 hours to that beginning 23:54, which was found to be suitable for the purpose of handling diurnal cycles within the model.

Brisbane's rainfall has strong inter-annual variability (Figure 2a). Klingaman et al. (2013) review what is known about the large-scale climate drivers of Queensland's seasonal and annual rainfall. The El Nino Southern Oscillation (ENSO) is known to be a strong influence particularly in spring (September-October) with La Nina years generally leading to wetter weather due to increased local sea surface temperatures. Colder phases of the Inter-decadal Pacific Oscillation strengthen the influence of La Nina, bringing the zone of heavy rainfall called South Pacific Convergence Zone closer to Queensland's coast. Synoptic influences affecting seasonal rainfall (Figure 2b) include blocking pressure systems in the Southern Ocean that affect the position of extra-tropical storm tracks, tropical cyclones and coastal depressions. Abbs and McInnes (2004) found five significant synoptic climate types driving extreme wet rainfall in south-east Queensland during summer (November-April), which are, in order of significance: high pressure systems to the south east of Australia, inland monsoonal troughs, two types of tropical cyclones, and a low pressure system over the Tasman Sea. Only the first two of these synoptic types were found to be significant for winter (May-October) extreme events. Diurnal variations in rainfall are also strong (Figure 2c), driven by convective circulation especially in the summer period October-March.

FIGURE 2 HERE

2.2 MDRC model estimation

The microcanonical MDRC is defined in Figure 1 based on the illustration in Olsson (1998). For a defined level of disaggregation, there is an interval with two sub-intervals of equal length. W_1 is the

proportion of the interval's rainfall volume R (mm) falling in the first sub-interval to give R_1 (mm), and W_2 is the proportion falling in the second sub-interval to give R_2 (mm). W_1 is calculated from the observed data as $W_1=R_1/R$ for each interval with a non-zero observed R. As rainfall volume is conserved at every level, $W_2=1-W_1$, and so the probability distribution of only W_1 needs to be defined. To reduce the effects of rainfall measurement tolerances, the W_1 values for intervals with trace rainfall, defined as R<0.3mm, were discarded. The probability distribution of W_1 is specified by the probabilities $P(W_1=0)$ and $P(W_1=1)$, where the former is the frequency with which $W_1=0$ and the latter is the frequency with which $W_1=1$, and the probability density function $p(W_1)$ that applies for $0<W_1<1$, which is taken to be a Beta distribution following Molnar and Burlando (2005). The probability density function of the Beta distribution is defined in Equation 1.

$$p(W_1 = x) = \frac{x^{\propto-1}(1-x)^{\beta-1}}{\mathrm{B}(\alpha,\beta)} \qquad (1)$$

where B is the beta function. The parameters, α and β, are estimated using the method of moments.

2.3 Parameter dependencies

The paper explores how $P(W_1=0)$, $P(W_1=1)$, α and β depend on: the cascade level; time of day; season; decade; rainfall volume; and the temporal structure of events. The W_1 values from all the available years in the period 1908-2015 are used at this stage. For each cascade level, the W_1 values are separated into sub-sets according to: 1) time of day (one sub-set for each hour, or a longer period for levels 1-5 where the interval size is greater than one hour); 2) month (one sub-set for each month); 3) R volume percentile (one sub-set for each 5% increment on the cumulative distribution function of R having excluded the trace values); and 4) event structure type, which following Olsson (1998) is either:

- The interval is surrounded by intervals with zero R (isolated, I)
- The interval is preceded by an interval with non-zero R and followed by an interval with zero R (preceded, P)
- The interval is preceded by an interval with zero R and followed by an interval with non-zero R (followed, F)
- The interval is surrounded by intervals with non-zero R (enclosed, E).

The values of $P(W_1=0)$, $P(W_1=1)$, α and β are estimated for each sub-set of data, and the variations between sub-sets are plotted. This is a univariate analysis in the sense that only one potential effect is controlled in each plot, and so additional plots explore potential interactions between effects. The analysis is then deepened by looking at the histograms of W_1 values over selected sub-sets of the data with the aims of identifying any effects on $p(W_1)$ not seen in the plots of α and β values and illustrating the level of suitability of the Beta distribution function.

A primary question, relevant to many downscaling applications, is the transferability of the model from a relatively short fitting period to a longer historical period. This question is first approached by exploring the decadal scale variations in the parameter estimates derived using each of the eight decadal scale periods delineated by vertical lines in Figure 2(a): 1908-1922; 1923-1935; 1936-1948; 1949-1961; 1961-1973; 1974-1986; 1987-2002; and 2003-2015. The different lengths of these periods allows for missing data so that each period has approximately the same number of rainfall observations. There is evidence in the literature that while daily extremes in eastern Australia are not increasing fine scale extremes are (Westra and Sisson 2011) and therefore it is expected that the downscaling parameters are changing. As well as looking for trends over time, the parameters are plotted against an ENSO index (Smith and Sardeshmukh 2000). Ideally the analysis would also seek to understand the dependence of the MDRC parameters on the synoptic scale weather system type driving the rainfall, for example the five synoptic climate types identified by Abbs and McInnes

(2004), with the view that these are potential physically-based predictors of the MDRC parameters (e.g. Groppelli et al. 2011). However, in our case, the lack of historic time-series data defining which system(s) is dominant at daily and sub-daily scales precludes this.

2.4 Model evaluation

Finally, an MDRC model fitted on the last period shown in Figure 2 (1987-2015) is evaluated both in that period and in an evaluation period (1908-1986). Alternative levels of model complexity (number of estimated parameters) are tested against observed data focussing on the extreme values of R and the time series autocorrelations. Because the fitted MDRC is a stochastic model, with each simulation based on random samples of W_1 from the fitted distributions, each simulation gives a different answer. Therefore 100 realisations are done, and model performance is judged on whether or not the observed rainfall statistic appears to be a sample from the distribution of simulated statistics, as represented by the 5^{th} and 95^{th} percentile values (estimated using the 6^{th} and 95^{th} highest values of the statistic out of the 100 realisations).

3 RESULTS AND DISCUSSION

3.1 Discard of data below the threshold

Applying the threshold of 0.3 mm led to 75, 83, 89, 92, 95, 96 and 98 % of the available W_1 values being discarded for cascade levels 1-7 respectively for the 1908-2015 period. Despite this, a large number of W_1 samples remain for the estimation of parameters (Tables A.1 and A.2).

3.2 Effects on $P(W_1=0)$ and $P(W_1=1)$

Figure 3 shows the diurnal, seasonal, volumetric and event structure effects on $P(W_1=0)$ and $P(W_1=1)$ for two representative cascade levels, 2 and 5 (representing the disaggregation from 12-hour to 6-hour intervals and from 90-minute to 45-minute intervals, respectively). Figures 3 (a, b) show that

the dry season is different from rest of the year, although whether the dry season is considered to be May-August, June-August or June-September depends on the cascade level, and is not generally synchronised with the typical seasonal variation of rainfall (Figure 2b). Figures 3 (c, d) show that diurnal effects are also small, with late morning and early afternoon quite consistently having the highest $P(W_1=0)$ and $P(W_1=1)$ values. Again, these are not synchronised with the typical diurnal variation in volume. The result for 09:00 in Figure 3(c) is almost certainly an artefact of the measurement method from the pre-tipping bucket era, when rolls of paper recording the pluviograph would be replaced at the start of the working day resulting in some accumulations over intervals. The 09:00 artefact was visible for levels 4, 5, 6 and 7 (90 mins to 11.25 mins); however it is not visible at any level when including only the high rainfall volumes, as used later for model evaluation, indicating that for practical purposes the problem is limited to the accumulation of small rainfall amounts. There was no visible variation in the parameter values over the seven days of the week. An important diurnal effect not shown in Figure 3 is for level 1, where it is less likely that a daily value of rainfall will be concentrated in the first part of the day ($P(W_1=1) = 0.24$ compared to $P(W_1=0) = 0.34$).

FIGURE 3 HERE

Figures 3 (e, f) show that volume effects on $P(W_1=1)$ and $P(W_1=0)$ are strong, with lower R more likely to be strongly disaggregated between the two sub-intervals at all levels. Unfortunately, these plots provide little information at extremely high R values, with only one estimate of $P(W_1=1)$ and $P(W_1=0)$ representing the wide range of rainfall in the 95 – 100 percentile range (for example, daily R varies from 43 to 311 mm in that percentile range). The limited number of samples discourages using smaller percentile ranges. The strong trend shown in Figures 3 (e, f) might be presumed to apply over the extreme values; or if a physical bound to R (a theoretical 100^{th} percentile on R for a given interval size) could be estimated then this R could not be concentrated further into a sub-

interval so that $P(W_1=0)$ would be zero, giving an intercept with the x-axis (100, 0). Figures 3 (g, h) confirm the results of Olsson (1998) and Guntner et al. (2001) that whether or not an interval falls within a longer event has a strong influence on the $P(W_1=0)$ and $P(W_1=1)$ values. Finally, on Figure 3, the choice of the trace rainfall threshold significantly affects the parameter estimates in the lower volume ranges. This is considered immaterial, so long as the estimates used are understood to be conditional on R>=0.3 mm and not used for applications where the distribution of R<0.3 mm across sub-intervals is relevant.

Figure 4 extends the analysis of Figure 3 by looking at the degree to which the diurnal, seasonal and structural effects are implicit in the volumetric effects on $P(W_1=0)$ and $P(W_1=1)$. Since the volume R is a function of hour of day, season and event length, it is reasonable to propose that these three variables have little effect on $P(W_1=0)$ and $P(W_1=1)$ that is independent of that volume, and therefore they do not need to be explicit in the model so long as the volume dependence is represented. However, Figure 4 shows that within the 5-percentile increments of volume there are consistent diurnal, seasonal and event structure effects. For example, Figure 4(a) implies that, for a given 12-hour rainfall volume, disaggregation into 6-hour volumes will generally be stronger (higher values of $P(W_1=0)$) if intervals over the whole day are taken into account rather than only those in the morning, which is consistent with the prevalence of shorter convective type events later in the day; and Figures 4(e and f) show that for a given rainfall volume there is generally weaker disaggregation (lower values of $P(W_1=0)$) if the interval is preceded by another wet interval. Therefore, the results shown in Figure 4 hint that there may be no simple, elegant MDRC model and instead all four types of effects – volume, time of day, month of year and event time structure - may need to be considered.

FIGURE 4 HERE

3.3 Effects on the Beta distribution parameters

Figure 5 repeats Figure 3 but for α and β. June-August is again the most distinguishable season considering all levels. The higher values of α and β in these months signify a lower variance in W_1, i.e. that R is more likely to be distributed evenly between two sub-intervals, which is consistent with the lower values of $P(W_1=0)$ and $P(W_1=1)$ in Figure 3. This encourages the segregation of these months from the other months so as not to underestimate the temporal spread of rainfall during these other months. Diurnal effects are weak and consistent with the results for $P(W_1=0)$ and $P(W_1=1)$ in Figures 3 (c,d). The strength of the volumetric effect in Figures 5 (e,f) contrasts with Figures 3 (e,f), with little variation of α or β above the 20-percentile for level 5 (and also levels 4, 6 and 7, not shown) and above the 50 percentile for level 2 (and also levels 1 and 3, not shown). The almost consistently higher values of α over β indicate negative skewness of $p(W_1)$ – another contrast with Figure 3, in which the generally higher values of $P(W_1=0)$ indicate a positive skewness. This and other interesting features of the data can be better discussed on viewing the shapes of the W_1 histograms.

FIGURE 5 HERE

The histograms in Figure 6 show the relative frequency of W_1 ($0<W_1<1$) as well as the values of $P(W_1=0)$ and $P(W_1=1)$ for all 7 levels. Following the importance of the event structure effect from Figures 3, 4 and 5, the histograms for the intervals that are categorised as I, P, F and E are presented separately. Category E, i.e. the fourth column of histograms in Figure 6, is the most important because the largest proportion of the events lie here (the proportions of intervals in the I, P, F and E categories are given in Table A.1). This column reflects results reported by Olsson (1998), with a normal-shaped distribution at the higher levels moving to a more uniform distribution at lower levels, and the values of $P(W_1=0)$ and $P(W_1=1)$ declining as level increases. Still referring to category E, the slight negative skewness (high W_1 is more frequent) over levels 1-4 means that it is more likely that most of R falls in the first sub-interval at fine scales. However, $P(W_1=0)$ is consistently higher

than $P(W_1=1)$ so that if all of R is in one sub-interval it is more likely to be the second. Again, this may be due to typical event profile: an event more likely to start suddenly and tail off than vice versa, so it is less likely for rainfall to be present in the first sub-interval and not in the second.

FIGURE 6 HERE

The first column in Figure 6 is the I category, comprising of a relatively small proportion of the total number of intervals considered. These histograms are positively skewed - because events tend to tail off as previously mentioned - with the exception of level 1, which is a special case because the diurnal pattern means there is high probability that all or much of R will fall in the afternoon. The second and third columns in Figure 6 illustrate that wet sub-intervals tend to cluster, for example there is a higher probability of high W_1 values if there is a preceding wet interval. At any level, the two distributions in the second and third columns of Figure 6 are approximately complementary, which means that $p(W_1)$ values for intervals in the P category are the same as $p(W_2)$ values for intervals in the F category. Consistent with this, the $P(W_1=0)$ values for the P category approximate the $P(W_1=1)$ values for the F category and vice versa. However close inspection of Figure 6 reveals that negative skewness values for the P category are of greater magnitude than the positive skewness for the F category, and this difference is consistent across levels, albeit small. This is presumably because of the time-structure of events previously explained.

Regarding event structure, it may be proposed that incorporating the general skewness of $p(W_1)$ and the general difference between $P(W_1=0)$ and $P(W_1=1)$ seen in Figures 4, 5 and 6, and the strong differences across the P and F categories seen in the same figures, will contribute to preserving the observed fine-scale structure of the rainfall. Whether this is useful in terms of performance will be tested later.

Figure 7 is in the same format as Figure 6, with the columns defined by R volume percentile categories, so that quartile 1 holds the intervals with the lowest 25 % of the above-trace R values for each level, etc. All the event structure categories are lumped together to produce Figure 7. Some of the general characteristics already seen in Figure 6 are repeated: the general positive skewness, the general observation that $P(W_1=0)>P(W_1=1)$, and the generally lower variance of $p(W_1)$ as level number increases. An exception to the latter observation is quartile 1, levels 1 to 3, where variance of $p(W_1)$ is less than it is for the higher levels. This means that the rainfall at 24-hour, 12-hour and 6-hour intervals is more evenly distributed over the interval if the rainfall volume is low. This effect is greater if only the lowest 5 % of volumes are included, and especially pronounced if only the data from the period 1999-2015 (the replacement gauge) are included resulting in a distinct peak at $P(W_1=0.5)$, a commonly observed anomaly (Licznar et al. 2015). This can be traced to very low values of rainfall being artificially distributed over the day. As initially shown by Figure 3, the differences between $p(W_1)$ across the three higher volume quartiles are small. Therefore, for identifying a MDRC model, it is likely to be sensible to neglect the W_1 values that originate from quartiles 1-3 considering that these quartiles contain volumes that are less important for most practical applications.

FIGURE 7 HERE

3.4 Transferability of the model across decades to generate long-term rainfall

The above analyses have lumped all available years from 1908 until 2015. To explore the potential inter-decadal variability, the data were divided into the decadal scale periods shown in Figure 2(a). Figures 8 (a-d) show the results for cascade levels 2 and 5. Since at least 1967, an upward trend exists in $P(W_1=0)$ and $P(W_1=1)$ from level 4 to level 7, consistent with the trends in extremes observed more generally over eastern Australia (Westra and Sisson 2011). The corresponding values of α and β also show an upward trend over the last 50 years, which means weaker disaggregation, somewhat cancelling the effect of the trend in $P(W_1=0)$ and $P(W_1=1)$. A similar result is found if only

the intervals in the upper quartile of volumes are used to estimate the parameters. The values of α and β for the period 1974-1986 were consistently high, which may be linked to the exceptionally high rainfall in 1974 (Figure 2a), and the occurrence of four strong La Nina years in that period. Figures 8(e-h) show the relationship between the parameters and an ENSO index (Smith and Sardeshmukh 2000) for levels 2 and 5. For these plots, the years have been assigned into ten different bands of ENSO strength, defined by the 10-percentile ranges from the sample cumulative distribution function, and the parameters estimated from the W_1 samples obtained from each band. At almost all levels α and β tend to decrease with increasing ENSO strength. Although this trend is consistent over levels, the p-statistics illustrate the limited significance of the linear trend for any individual level. Noting that El Nino years tend to be drier in Brisbane, the trends in Figures 8(e-h) are consistent with the volume-dependence of the parameters previously discussed. A plot (not shown) similar to Figure 5 indicates that ENSO may have a small effect that is independent of volume, with strong La Nina years leading to less rainfall disaggregation, however it is too small to be conclusive. For the purpose of developing a MDRC model it is therefore assumed that any effect of ENSO on the scaling properties can be included by means of a volume dependence.

FIGURE 8 HERE

The results of the analysis provide guidance for defining a baseline MDRC model. It is assumed that the model would be employed for a continuous time approach to flood risk estimation and therefore achieving a realistic time-distribution of high R values is the aim. The baseline model is:

- A Beta distribution is assumed for ($0<W_1<1$), and symmetry is not assumed, so there are four parameters: $P(W_1=1)$, $P(W_1=0)$, β and α.
- These parameters are estimated using the data from only the upper quartile of volume (having previously excluded the trace values) at each level (R > 11.0, 8.4, 6.0, 4.4, 3.2, 2.2, 1.6 mm for levels 1-7 respectively);

- A separate parameter set is estimated for each event structure type, I, F, P and E, and for each cascade level.
- The parameters are otherwise assumed constant over the decades, months and time of day.

This means that 16 parameters are estimated for each level. The evaluation will include testing simplifications to this baseline model. The model is fitted using the period from 1987-2015, leaving the period 1908-1987 as an evaluation period. The fitting period aims to represent the relatively short length of sub-daily data that may be available in practice; while the longer evaluation period tests the model's ability to extend the sub-daily record over long periods under a variable and potentially changing climate (noting from Figure 2 that the most extreme high and low annual rainfalls are in the evaluation period). The parameter estimates and the numbers of samples (intervals) used for the initial model are in Tables A.2 and A.3.

Since the assumed application of the model is flood risk estimation, the evaluation focuses first on the higher percentiles of R. Figure 9 shows the frequencies of observed and simulated R considering only the highest 2.5% (having previously excluded the trace values) of observed R for selected levels, including results from both the fitting (a, c, e, g) and evaluation (b, d, f, h) periods. The frequencies on the y-axes of Figure 9 are given relative to number of observed R so that any bias in the simulated results can be seen. The vertical lines through the bars represent the 5^{th} and 95^{th} percentiles from the 100 simulations, and the dashed vertical lines show the magnitude of some notable historical point rainfalls gauged in New South Wales and Queensland, as additional indicators of the plausibility of the simulated extremes. Although the performance of the model shown in Figure 9 is considered good given that many known effects on the parameters are neglected or simplified, Figures 9(b, d, f, h) show that in the evaluation period the rainfall volumes are over-estimated at cascade level 3 and this propagates to the higher levels. Plotting the mean, standard deviation and skewness of the observed and simulated rainfall within the same range of volumes also exhibits this bias. The direction of this bias is consistent with over-estimating the strength of disaggregation,

which is expected considering that the parameters were estimated using the W_1 samples representing the upper 25 % of rainfall volumes whereas the evaluation uses the upper 2.5 %. Using only the upper 2.5 % for parameter estimation does not improve performance due to the low number of samples in the fitting period. This supports the view that the trends in Figures 3, 4 and 5 could be explored further with the aim of developing more robust parameter estimates for extreme high volumes. Comparing the performance in the fitting and evaluation period implies that the principal cause of the bias may be transferring the parameters from the recent fitting period to earlier decades. .However, if the model is fitted and evaluated using the data from the period 1908-1986, the over-estimation of extreme rainfall does not visibly improve, so it is concluded that indeed the volume dependence of parameters is the principal performance issue and this is exaggerated in the 1908-1986 period due to the more extreme daily rainfall included in that period.

FIGURE 9 HERE

As well as the volume frequency distribution, the time series of volumes (the pluviograph) is relevant for many applications, for example rainfall-runoff modelling. Figure 10 shows the autocorrelation structure of the simulated rainfall, again excluding from the calculation any interval that is not in the upper 25 % by rainfall volume, compared to the equivalent using the observed rainfall. The upper 25 % is used rather than the upper 2.5% that was used in Figure 9 because of the lower number of samples available to estimate the autocorrelation structure (one sample consists of a pair of R values, both of which are above the 25 percentile value, which considerably reduces the number of samples especially at the larger lags). Like Figure 9, the vertical lines through the bars represent the 5^{th} and 95^{th} percentiles from 100 simulations. Figure 10 shows that the modelled autocorrelation structures may be considered realistic, although there is a tendency to over-estimate the autocorrelations. This is not easy to interpret but may be due to the simple event structure categorisation, which is based only on the presence or not of rainfall in the surrounding interval

rather than the real structural complexity of storm cells at sub-interval time-scales. The lower variance of estimates in the evaluation period compared to the fitting period is because of the larger number of samples in the former.

FIGURE 10 HERE

Table 1. Observed and simulated probability of changing from low to high volumes (as defined by upper 25 percentile of rainfall volumes) from one interval to the next

Level	25 percentile (mm)	Probability	Observed	Simulated
2	6.0	P(low-low)	0.51	0.52
		P(low-high)	0.17	0.18
		P(high-low)	0.18	0.16
		P(high-high)	0.14	0.11
5	2.2	P(low-low)	0.53	0.53
		P(low-high)	0.11	0.14
		P(high-low)	0.17	0.16
		P(high-high)	0.20	0.18

A limitation of the autocorrelation structure as a performance metric is that it does not describe how accurately the model captures the fluctuation of rainfall from values outside (or inside) the upper 25 % range to inside (or outside). Therefore, to complement Figure 10, Table 1 evaluates the frequency with which the rainfall volume enters, exits or stays within that range from one interval to the next in the evaluation period. The results show good accuracy, and the model's slight overestimation of

the probability that rainfall will stay in the high range is consistent with the over-estimation of autocorrelation shown in Figure 10.

A question of interest is whether a simpler model can produce equally realistic results. Figure 11 shows that $P(W_1=0)$ and $P(W_1=1)$ have similar values for the E and I categories of event. Figure 11 also shows a less strong, but still good, correspondence between the α and β values. Therefore, a simpler parameterisation was tested, which neglected the event structure and assumed a symmetrical distribution of W_1 values so that $P(W_1=0) = P(W_1=1)$ and $\alpha = \beta$. Hence this simpler model only requires that two parameters are estimated per cascade level compared with the baseline model's 16. The performance of the simpler model in terms of extreme value frequencies (Figure A.1) was also considered to be good, with the over-estimation of frequencies increasing visibly only at time intervals 12, 6 and 3 hours. This can be explained by the high values of $P(W_1=0)$ and $P(W_1=1)$, low values of α and β, and asymmetry that are associated with event structure categories I, P and F (Figures 3, 5 and 6) that tend to increase the level of disaggregation, whereas the high volume events are more dominated by category E (Table A.2). The mean values of simulated rainfall for the evaluation period are higher than the observed values by 7.2 %, 17 %, 16 % and 20 % for the 12-hour, 3-hour, 45-minute and 11.25-minute intervals respectively, compared to corresponding overestimations of 6.2 %, 16 %, 18 % and 25 % obtained using the original, less parsimonious model. These comparisons include only the highest 2.5 % of volumes as show in Figures 9 and A1. As previously noted, the aim is for the observed values to be samples from the distribution of simulated values so these overstimations should be interpreted considering the uncertainty intervals shown in the figures. The reduction in the autocorrelation performance was also small but noticeable (Figure A.2). The small loss in autocorrelation performance is surprising considering the generally strong dependence of parameters on the time series properties as represented by the event structure categories and asymmetry in the W_1 distribution (Figures 3-7); however the focus on the upper quartile of volumes in the autocorrelation analysis moderates this dependence.

FIGURE 11 HERE

A further simplification of the model was achieved by empirically relating the parameters to the cascade level. Figure 12(a) shows the relationship between the value of $P(W_1=0)$, as estimated from the two-parameter-per-level model, and the cascade level; and Figure 12(b) shows the relationship between the same values of $P(W_1=0)$ and the corresponding values of the natural logarithm of α. The two regression equations derived from these figures are:

$$p = 0.176 - 0.0215 \times L \qquad (2)$$

$$\ln(\alpha) = 0.805 - 8.36 \times p \qquad (3)$$

where p is the probability $P(W_1=0)$ and L is the cascade number from 1 to 7. Combining these two equations α can also be estimated from the cascade level:

$$\ln(\alpha) = -0.664 + 0.180 \times L \qquad (4)$$

which is the line in Figure 12(c). Deriving (4) by combining (2) and (3) rather than regressing ln(α) against L aims to maintain as closely as possible the dependency between $P(W_1=0)$ and α. Hence this version of the model has a total of four parameters, which are the four regression coefficients in (2) and (3). As expected from the low residuals seen in Figure 12, the performance of this model is apparently identical to the results in Figures A1 and A2, with relative biases of 7.8 %, 16 %, 17 % and 20 % for the 12-hour, 3-hour, 45-minute and 11.25-minute intervals almost identical to those reported previously for the two-parameter-per-level model.

The exploitation of scaling properties in this way has the same advantage as the canonical approach to MDRC modelling in terms of the low number of parameters and potential to extrapolate to unobserved scales, but without the theoretical encumbrances as reviewed earlier in the paper.

FIGURE 12 HERE

In summary, the losses of performance caused by the model simplifications illustrate the benefit of explicitly including the categories I, P, F and E and asymmetry of the W_1 distribution in the parameterisation, and this conclusion is expected to apply to other application types as well as extreme high volumes. However, if a more parsimonious parameterisation is sought, for example for regionalising parameters across multiple sites and including spatial dependence or extrapolating to unobserved time-scales (Onof et al. 2005, Thober et al. 2014), the results show that this can be achieved with small sacrifice of performance.

4 CONCLUSION

The first aim of this research was to determine how rainfall scaling properties, represented by the parameters of a microcanonical MDRC model (using a Beta distribution allowing for intermittency of rainfall), can vary over: cascade level; diurnal, seasonal and decadal scales; event structure; rainfall volume; and an ENSO index. In some respects the results substantiate the previous results of Olsson (1998), Guntner et al. (2001), Molnar and Burlando (2005) and Rupp et al. (2009) who between them found significant dependencies on event structure, season and rainfall volume; and Licznar et al. (2015) who illustrated the potential for parameter bias due to climate oscillations within a 25-year period. Another result in common with previous papers is the relative consistency of the downscaling parameters from daily scale to around 45 minutes, then greater changes from 45 minutes to ~10 minutes. This result has been associated with physical structure of storms and storm

cells (Onof et al. 1996). Extending the scope of previous literature on microcanonical MDRC modelling, the results showed that there are significant diurnal effects associated with convective cycles; and some evidence of long-term decadal scale non-stationarity, with strength of disaggregation to the finer resolutions (< 90 mins) increasing in recent decades. ENSO was not found to be an important effect on the downscaling parameters except through its effect on rainfall volumes.

The second aim of the paper was to evaluate the performance of the MDRC model for replicating observed statistics of extreme high rainfall. The evaluation used a fitting period (1987-2015) and an evaluation period (1908-1986). The model was fitted for each cascade level independently and included only the principal effects on parameter values, which were rainfall volume and event structure category. The performance (e.g. Figures 9 and 10) was considered good, although there was some bias towards simulating higher frequencies of a given extreme value than observed in the evaluation period. Moving to a simpler model that excluded the event structure category and assumed symmetrical probability distributions resulted in small loss of performance in terms of volume frequency analysis and in terms of autocorrelations (Figures A.1, A.2). An even simpler model with only four parameters, which exploited empirically derived relationships between the parameters and the cascade level, resulted in indetectable further loss of performance. A challenge for improving the extreme value model performance is extrapolating the general volume dependence of parameters to the high extremes, where there are too few data to estimate the parameters. An approach to improving the extreme value performance would be to bring in more data by spatially generalising the model (e.g. Westra and Sisson 2001). This may also permit the synoptic climate controls on the parameters to be identified, which may provide more confidence if extrapolating the model to future climate conditions.

ACKNOWLEDGEMENTS

This work was partly funded by Neil McIntyre's Australian Research Council Future Fellowship Award FT140100977 and Meng Shi's Department of Education's Australian Postgraduate Award.

REFERENCES

Abbs, D.J. and McInnes, K.L. 2004. The impact of climate change on extreme rainfall and coastal sea levels over south-east Queensland, Part 1: Analysis of Extreme Rainfall and Wind Events in a GCM. CSIRO Atmospheric Research, November 2004, PMB No 1, Aspendale, Victoria, 3195, 47 pp.

Deidda, R., Benzi, R. and Siccardi, F, 1999. Multifractal modeling of anomalous scaling laws in rainfall. Water Resources Research, 35 (6), 1853– 1867

Groppelli, B., Bocchiola, D. and Rosso, R. 2011. Spatial downscaling of precipitation from GCMs for climate change projections using random cascades: A case study in Italy. Water Resources Research, 47, W03519, doi:10.1029/2010WR009437

Güntner, A., Olsson, J., Calver, A., and Gannon, B. 2001. Cascade-based disaggregation of continuous rainfall time series: the influence of climate. Hydrology and Earth System Sciences, 5, 145-164, doi:10.5194/hess-5-145-2001, 2001

Klingaman, N.P., Woolnough, S.J. and Syktus, J. 2013. On the drivers of inter-annual and decadal rainfall variability in Queensland, Australia. International Journal of Climatology, 33, 2413–2430

Licznar, P., De Michele, C. and Adamowski, W. 2015. Precipitation variability within an urban monitoring network via microcanonical cascade generators. Hydrology and Earth System Sciences, 19, 485–506. doi:10.5194/hess-19-485-2015

Lovejoy, S. and Schertzer, D. 2013. The Weather and Climate. Emergent Laws and Multifractal Cascades. Cambridge University Press, Cambridge.

Olsson, J. 1998. Evaluation of a cascade model for temporal rainfall disaggregation. Hydrology and Earth System Sciences, 2, 19–30.

Onof, C., Chandler, R.E., Kakou, A., Northrop, P., Wheater, H.S. and Isham, V. 2000. Rainfall modeling using Poisson-cluster processes: a review of developments. Stochastic Environmental Research and Risk Assessment, 14, 384– 411

Onof, C., Northrop, P., Wheater, H. S. and Isham, V. 1996. Spatiotemporal storm structure and scaling property analysis for modelling. Journal of Geophysical Research: Atmospheres, 101 (D21), 26415-26425

Onof, C., Townend, J. and Kee, R. 2005. Comparison of two hourly to 5-min rainfall disaggregators. Atmospheric Research, 77, 176– 187

Rupp, D. E., Keim, R. F., Ossiander, M., Brugnach, M., Selker, J.S. 2009. Time scale and intensity dependency in multiplicative cascades for temporal rainfall disaggregation. Water Resour. Res., 45, W07409, doi:10.1029/2008WR007321.

Sivakumar, B. and Sharma, A. 2008. A cascade approach to continuous rainfall data generation at point locations. Stochastic Environmental Research and Risk Assessment, 22, 451–459

Smith, C.A. and Sardeshmukh, P. 2000. The effect of ENSO on the intraseasonal variance of surface temperature in winter. International Journal of Climatology, 20, 1543-1557

Thober, S., Mai, J., Zink, M. and Samaniego, L. 2014. Stochastic temporal disaggregation of monthly precipitation for regional gridded data sets, Water Resour. Res., 50, 8714–8735, doi:10.1002/2014WR015930

Westra, S. and Sisson, S. 2011. Detection of non-stationarity in precipitation extremes using a max-stable process model. Journal of Hydrology, 406, 119–128,doi:10.1016/j.jhydrol.2011.06.014.

APPENDIX A

Table A.1 Proportions of the intervals in each structural category in the period 1908-2015, having removed all values below the 0.3 mm threshold

Structural category	Level						
	1	2	3	4	5	6	7
I	0.22	0.22	0.17	0.13	0.10	0.06	0.03
P	0.23	0.31	0.20	0.19	0.16	0.13	0.09
F	0.25	0.23	0.23	0.22	0.20	0.18	0.14
E	0.30	0.33	0.39	0.46	0.54	0.63	0.74

Table A.2 Number of intervals in the fitting period, 1987-2015, used to estimate each parameter

Parameter	Structural category	Level						
		1	2	3	4	5	6	7
$P(W_1=0)$ & $P(W_1=1)$	I	63	82	93	106	104	91	53
	P	70	89	103	118	148	170	190
	F	129	154	204	251	301	315	358
	E	229	323	461	681	1019	1562	2288
α & β	I	27	48	51	58	67	71	47
	P	45	59	78	88	114	138	167
	F	69	86	125	153	200	221	281
	E	199	288	419	629	968	1521	2263

Table A.3 Parameter values estimated from fitting period, 1987-2015

Parameter	Structural category	Level						
		1	2	3	4	5	6	7
$P(W_1=0)$	I	0.41	0.22	0.20	0.25	0.19	0.10	0.06
	P	0.16	0.08	0.07	0.03	0.05	0.02	0.00
	F	0.45	0.36	0.35	0.35	0.31	0.29	0.21
	E	0.09	0.06	0.05	0.04	0.03	0.02	0.01
$P(W_1=1)$	I	0.16	0.20	0.25	0.21	0.16	0.12	0.06
	P	0.20	0.26	0.17	0.22	0.18	0.17	0.12
	F	0.02	0.08	0.03	0.04	0.02	0.01	0.00
	E	0.04	0.05	0.04	0.04	0.02	0.01	0.00
α	I	0.58	0.69	0.93	0.56	0.87	0.70	1.02
	P	0.64	0.75	1.32	1.27	1.09	1.72	2.47
	F	0.58	0.58	0.56	0.58	0.74	0.68	0.82
	E	0.67	0.89	1.04	1.33	1.63	2.04	2.73
β	I	0.90	0.30	0.42	0.34	0.57	0.59	1.02
	P	0.45	0.41	0.57	0.54	0.54	0.63	0.74
	F	0.78	0.56	0.69	0.72	1.12	1.28	1.94
	E	0.74	0.86	1.06	1.28	1.50	1.89	2.56
$P(W_1=0)$	-	0.15	0.13	0.11	0.10	0.07	0.04	0.02
α	-	0.67	0.72	0.85	0.99	1.24	1.49	1.95

The last two rows are values estimated using the two-parameter-per-level model

FIGURE A.1 HERE

FIGURE A.2 HERE

FIGURE CAPTIONS

Figure 1. Schematic of the employed MDRC, where daily data are disaggregated into 11.25 minute data using seven cascade levels (adapted from Olsson 1998)

Figure 2. Inter-annual, seasonal and diurnal variability of rainfall amounts

Figure 3. Seasonal, diurnal, volumetric and event structure effects on $P(W_1=0)$ and $P(W_1=1)$ for levels 2 and 5

Figure 4. The interactions between volumetric effects and other effects on $P(W_1=0)$ for levels 2 and 5

Figure 5. Seasonal, diurnal, volumetric and event structure effects on Beta distribution parameters for levels 5 and 2

Figure 6. Histograms showing relative frequency of W_1 in ten bins and values of $P(W_1=0)$ and $P(W_1=1)$ for all 7 levels and the four event structure categories

Figure 7. Histograms showing relative frequency of W_1 in ten bins and values of $P(W_1=0)$ and $P(W_1=1)$ for all 7 levels. The data are separated into: Quartile 1 (intervals with lowest 25 % of non-zero volumes) to Quartile 4 (intervals with highest 25 % of non-zero volumes). Dots show the probability mass calculated from a Beta distribution that is fitted (method of moments) for each level using only the upper 50 percentile of volumes

Figure 8. Decadal scale variation in $P(W_1=0)$, $P(W_1=1)$, α and β, and their relations with ENSO anomaly

Figure 9. Frequencies of observed and simulated R in the fitting (a, c, e, g) and evaluation (b, d, f, h) periods including only the R values within the upper 2.5 % of observed volume for each interval duration. Both observed and simulated frequencies are given relative to number of observed R. Simulated R is range defined by upper and lower 5 percentile from 100 realisations. HNPR=Historical Notable Point Rainfall based on long-term records across Queensland and New South Wales from http://www.bom.gov.au/water/designRainfalls/rainfallEvents/ausRecordRainfall.shtml

Figure 10. Observed and simulated autocorrelation structures in the fitting (a, c, e, g) and evaluation (b, d, f, h) periods including only the R values within the upper 25 % by volume for each interval duration. Simulated R is range defined by upper and lower 5 percentile from 100 realisations.

Figure 11. Relationship between: a) P(W1=0) and P(W1=1); and b) alpha and beta for each event structure category

Figure 12. Relationships between: a) P(W1=0) and the cascade level; b) alpha and P(W1=0); and c) alpha and the cascade level. All relationships are for the two-parameter-per-level model

Figure A.1. Equivalent to Figure 9 but when the event structure and asymmetry are not considered in the parameterisation (2 parameters per level instead of 16)

Figure A.2. Equivalent to Figure 10 but when the event structure and asymmetry are not considered in the parameterisation (2 parameters per level instead of 16)

Figure 1

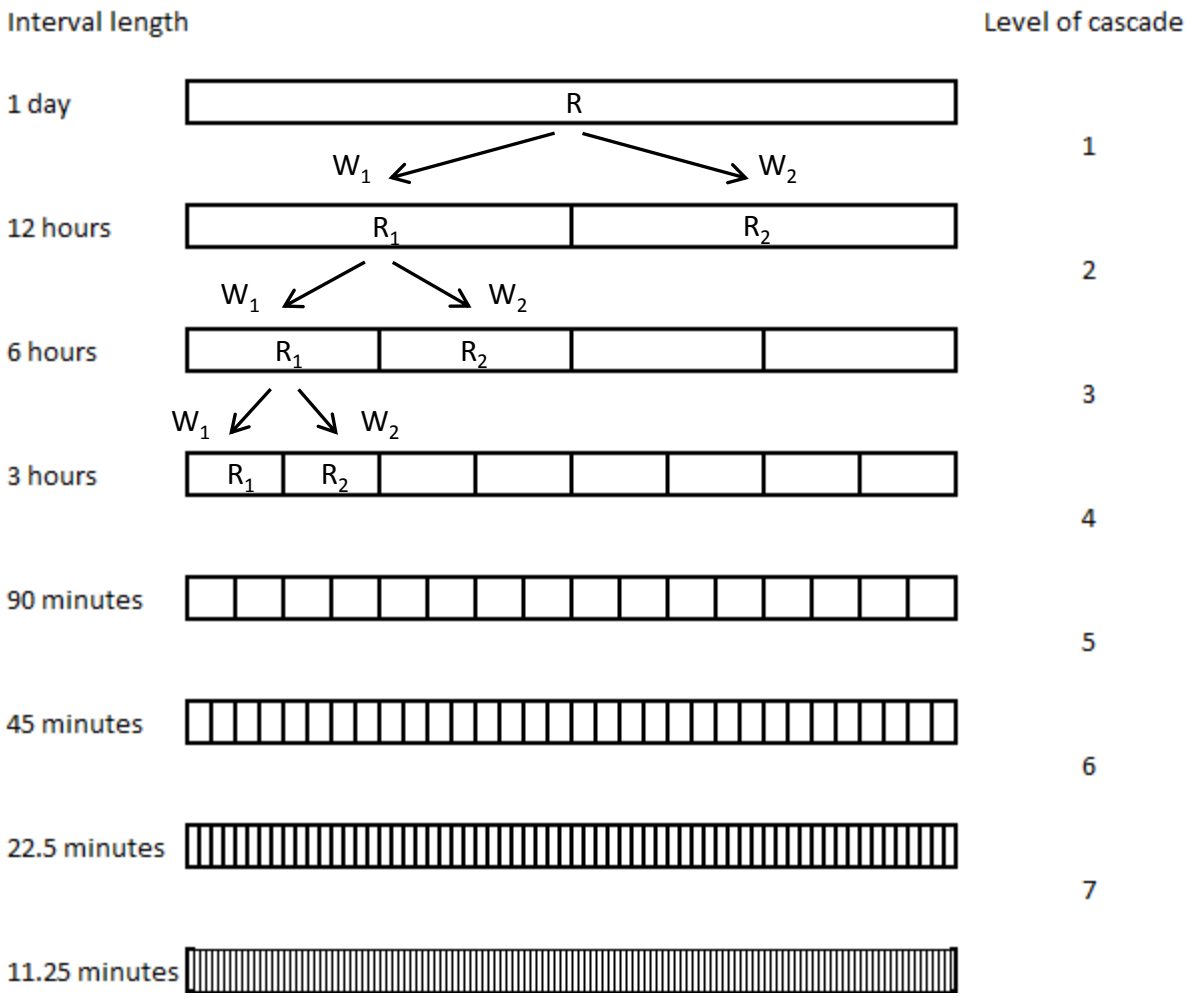
Interval length
Level of cascade
1 day
R
1
W1
W2
12 hours
R1
R2
2
W1
W2
6 hours
R1
R2
3
W1
W2
3 hours
R1
R2
4
90 minutes
5
45 minutes
6
22.5 minutes
7
11.25 minutes

Figure 2

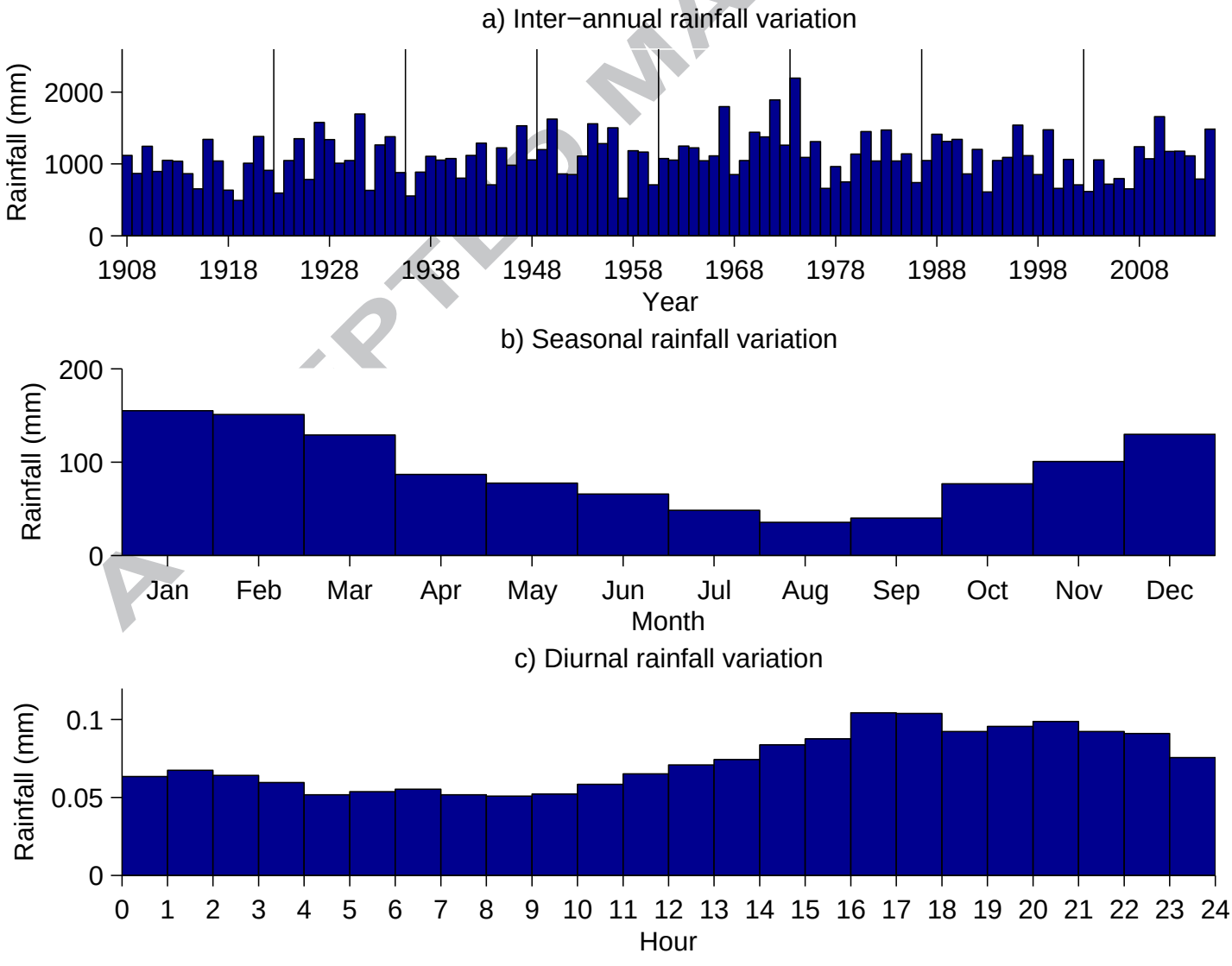

Figure 3

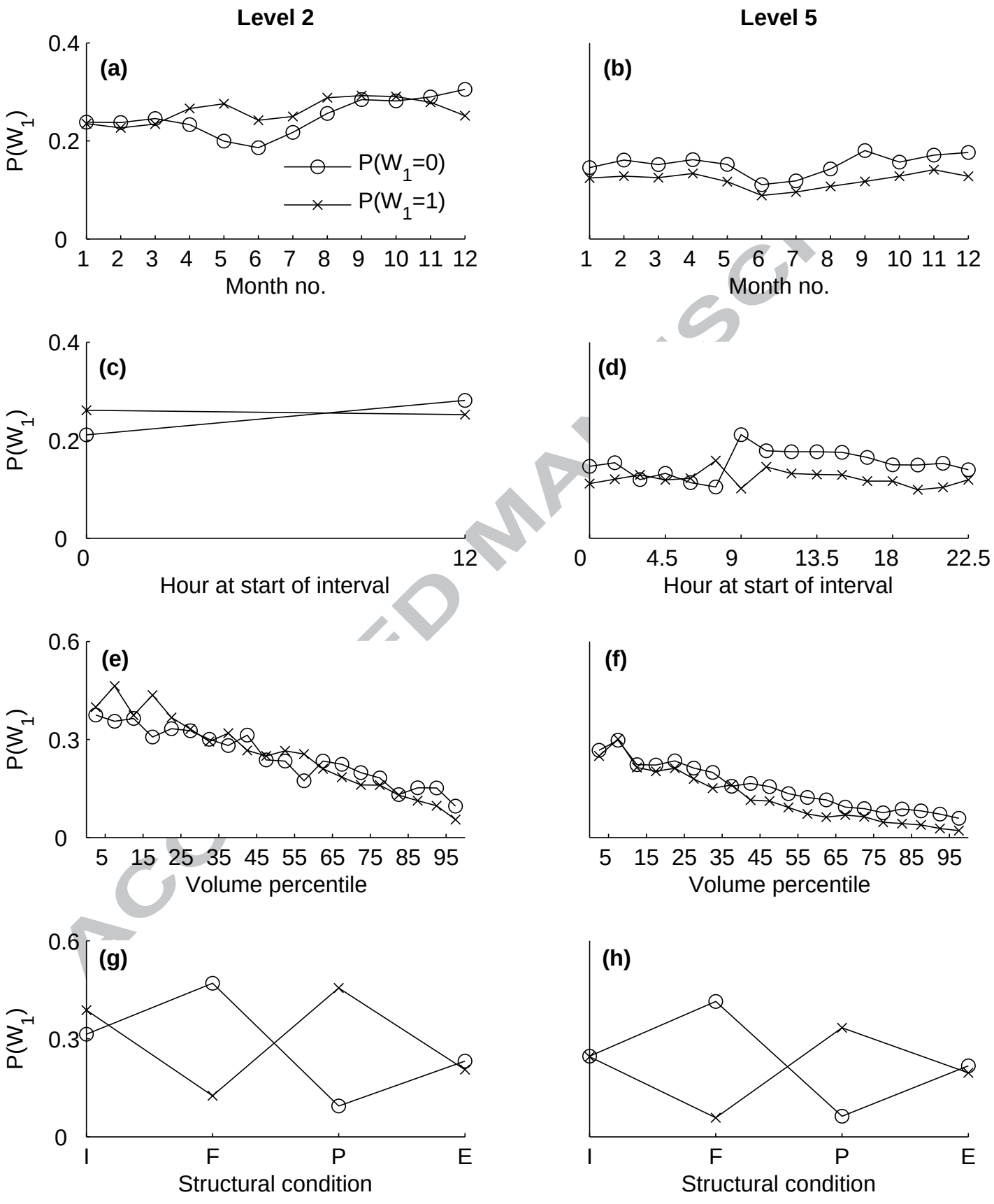

Figure 4

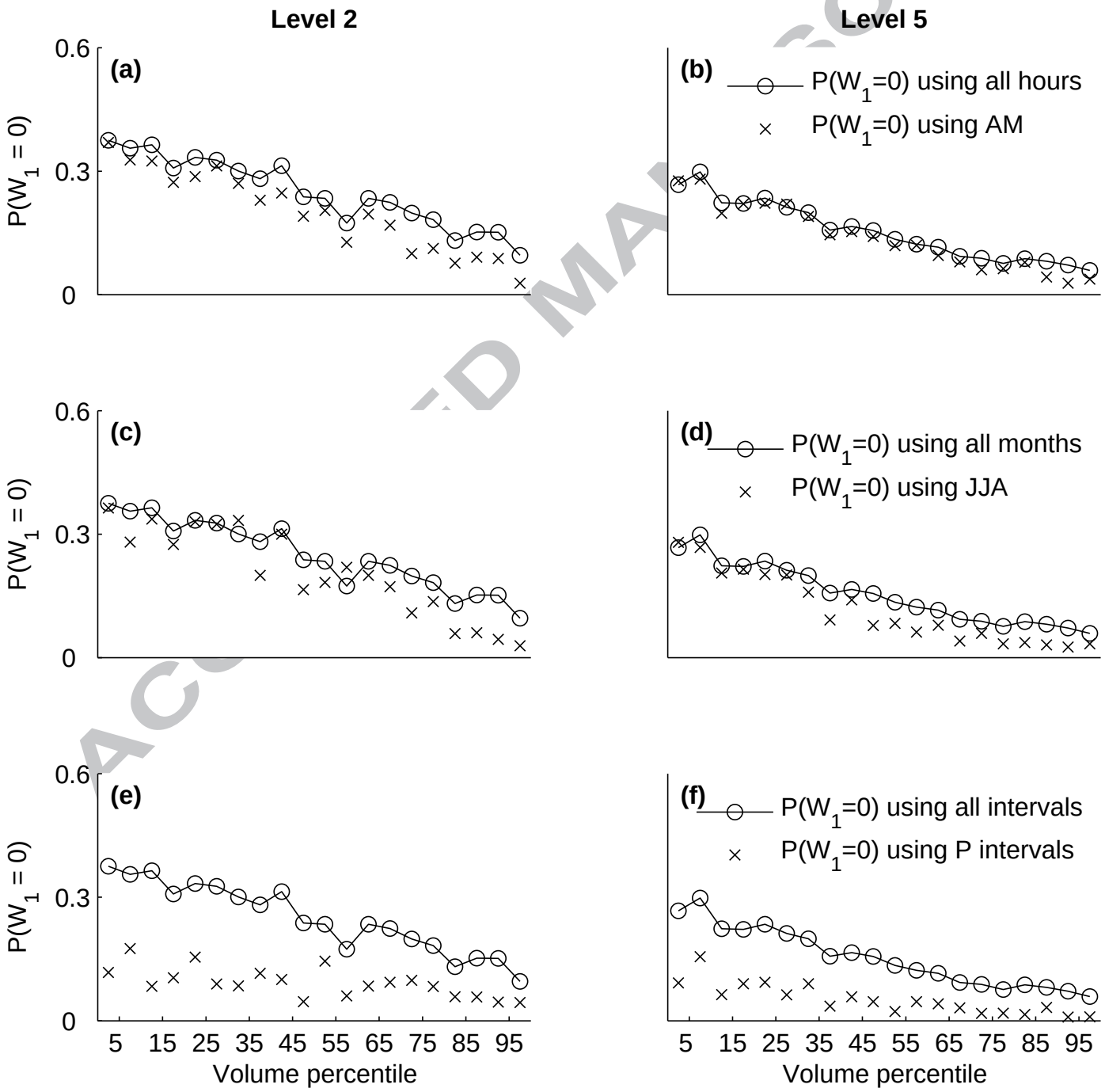

Figure 5

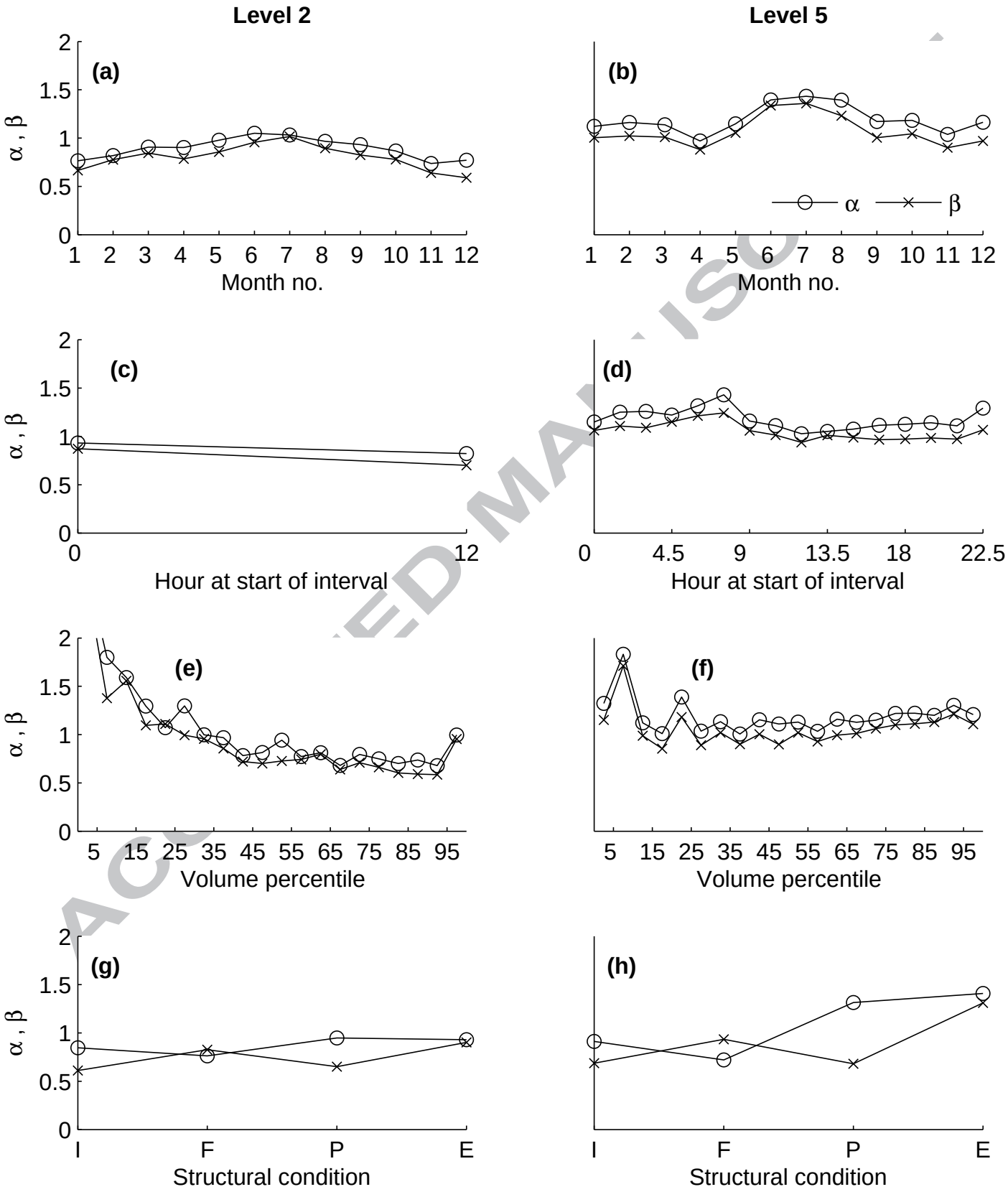

Figure 6

Figure 7

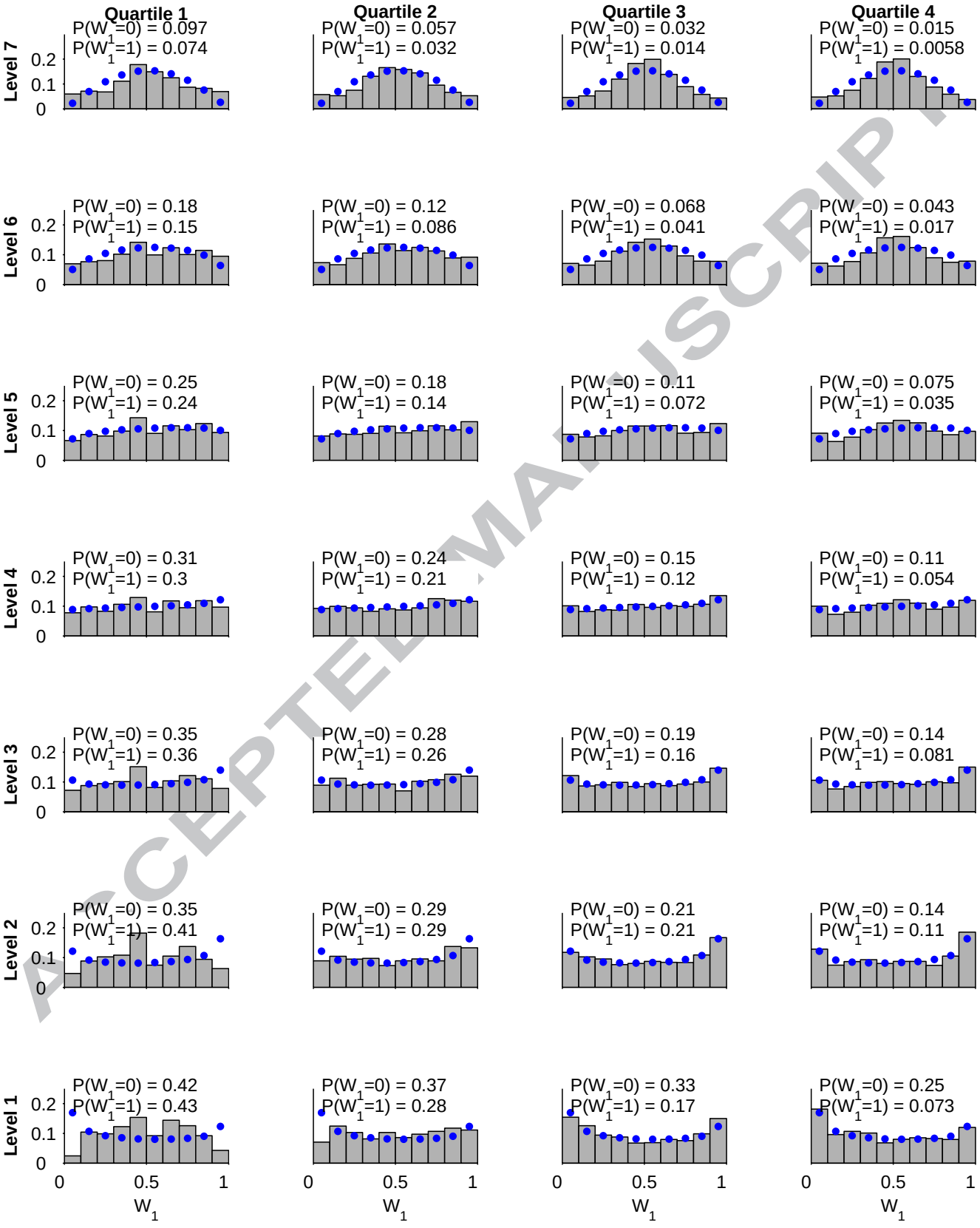

Figure 8

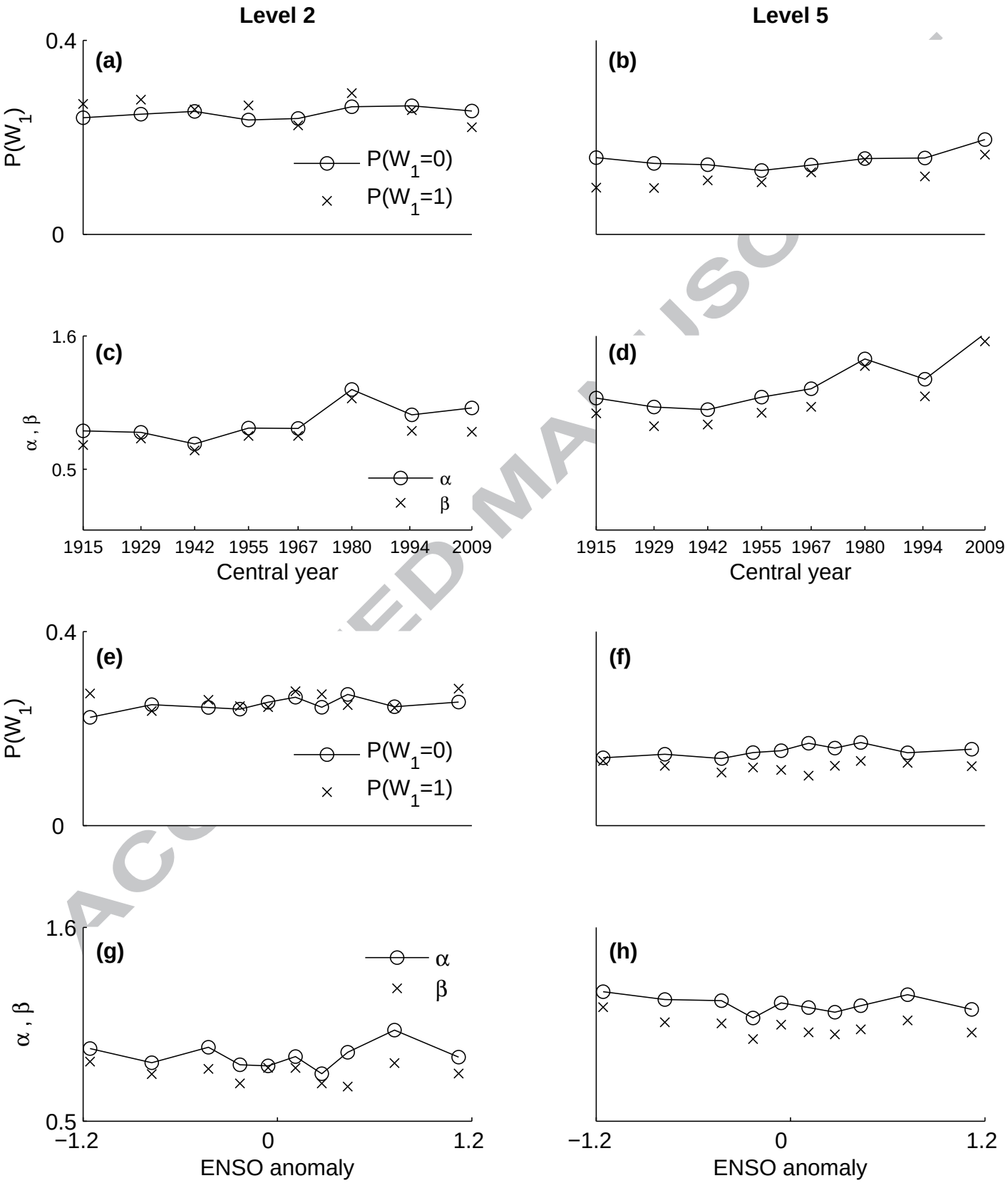

Figure 9

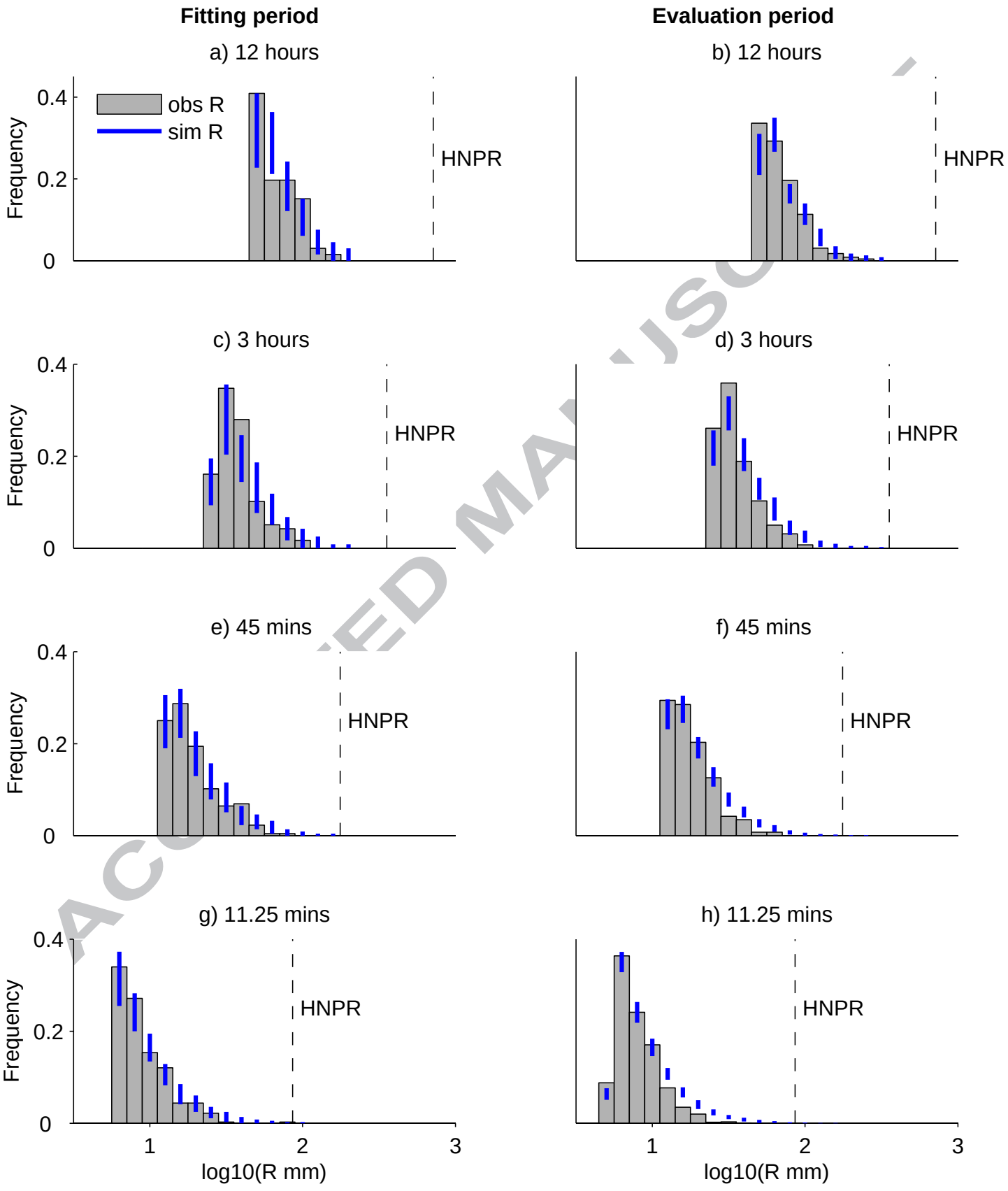

Figure 10

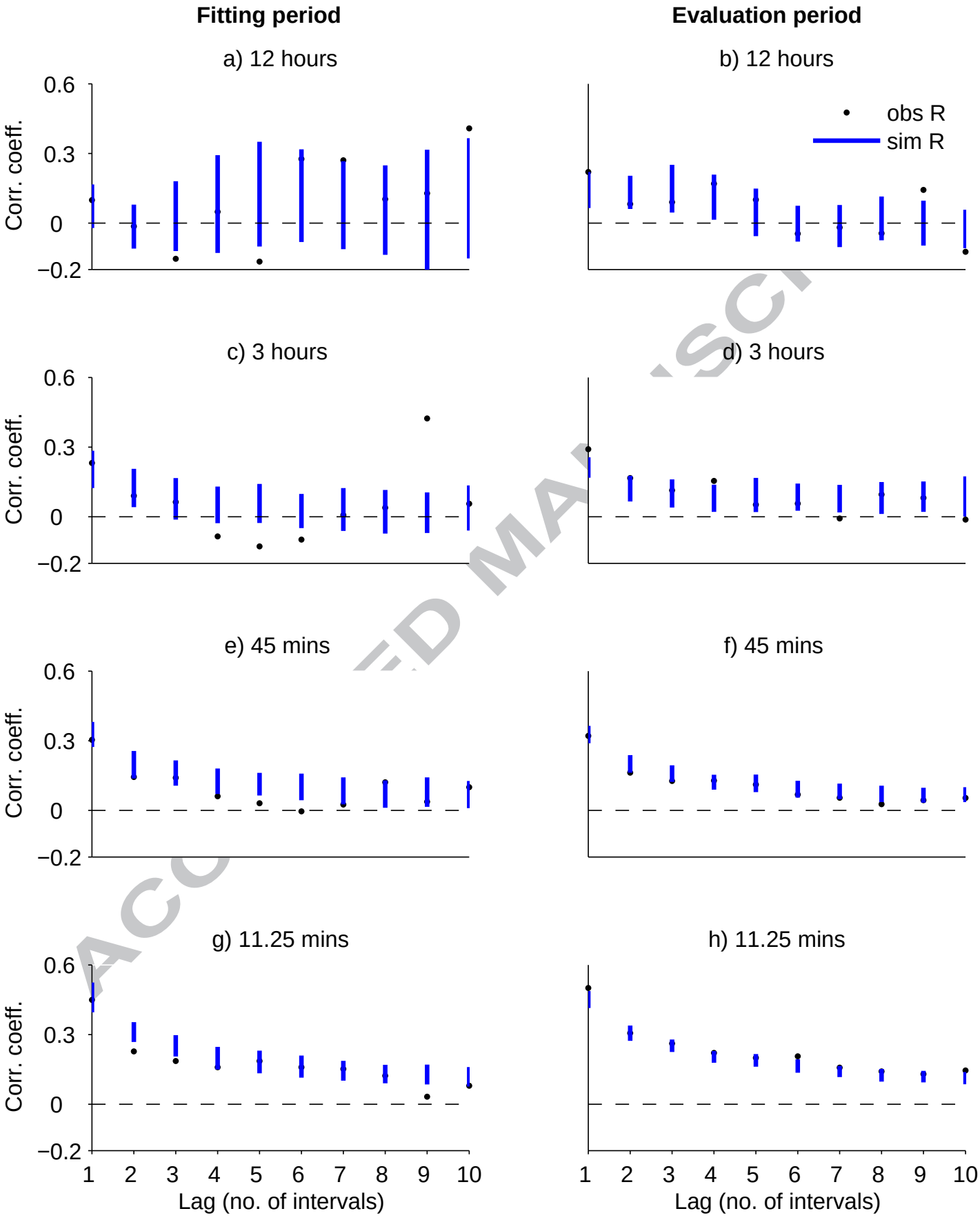

Figure 11

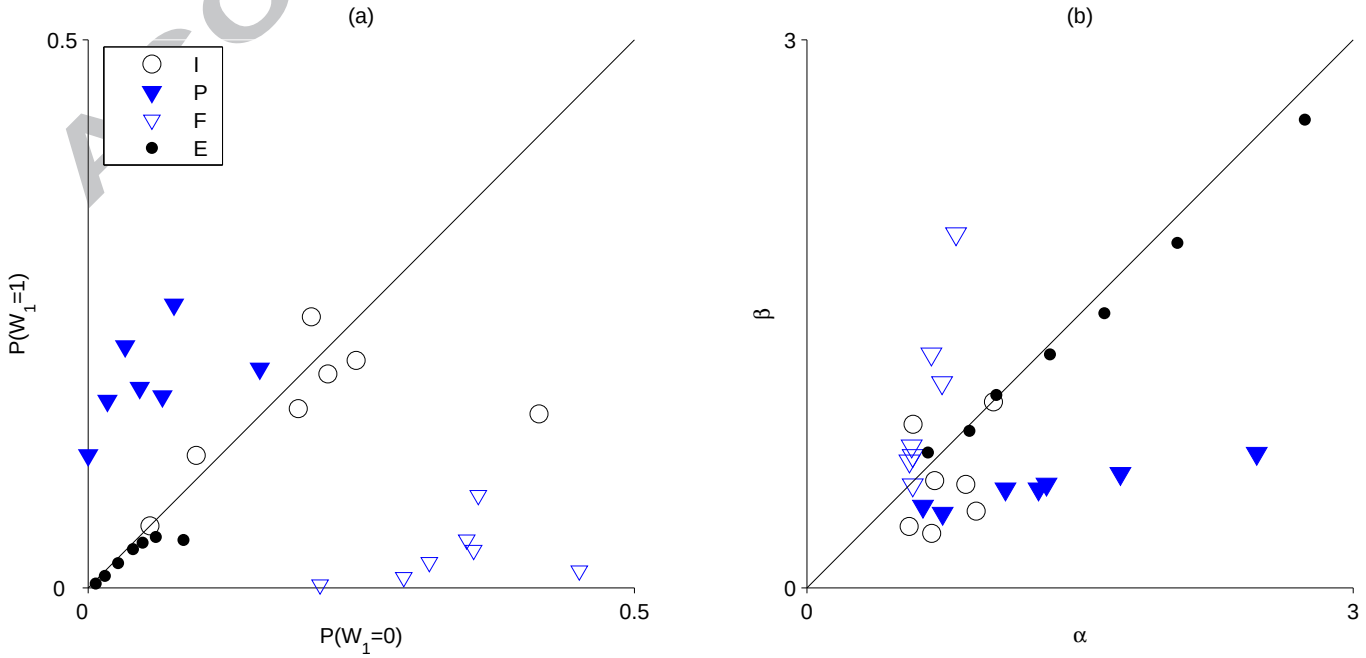

Figure 12

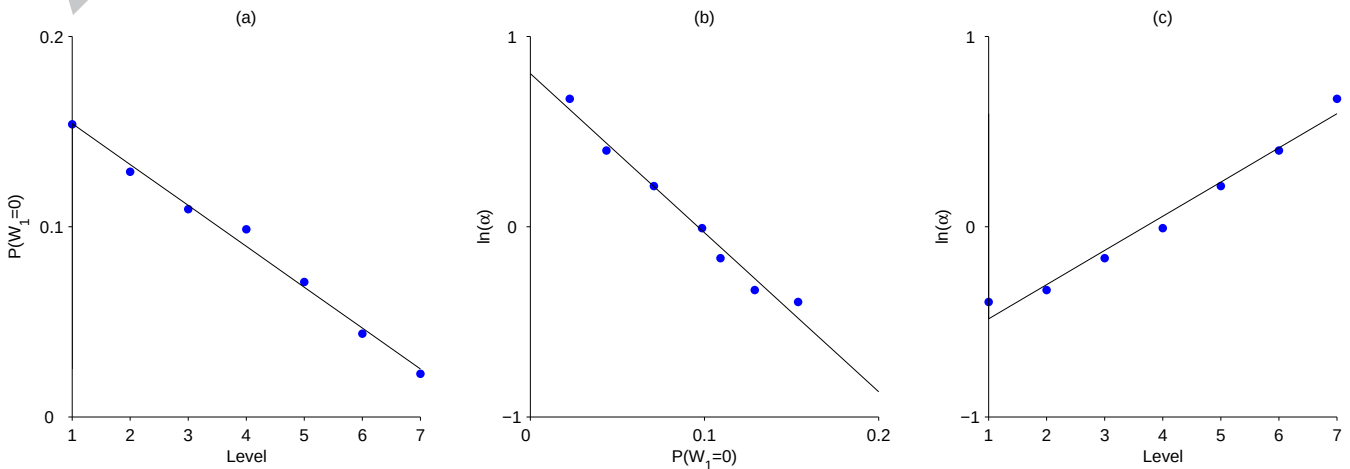

Figure A.1

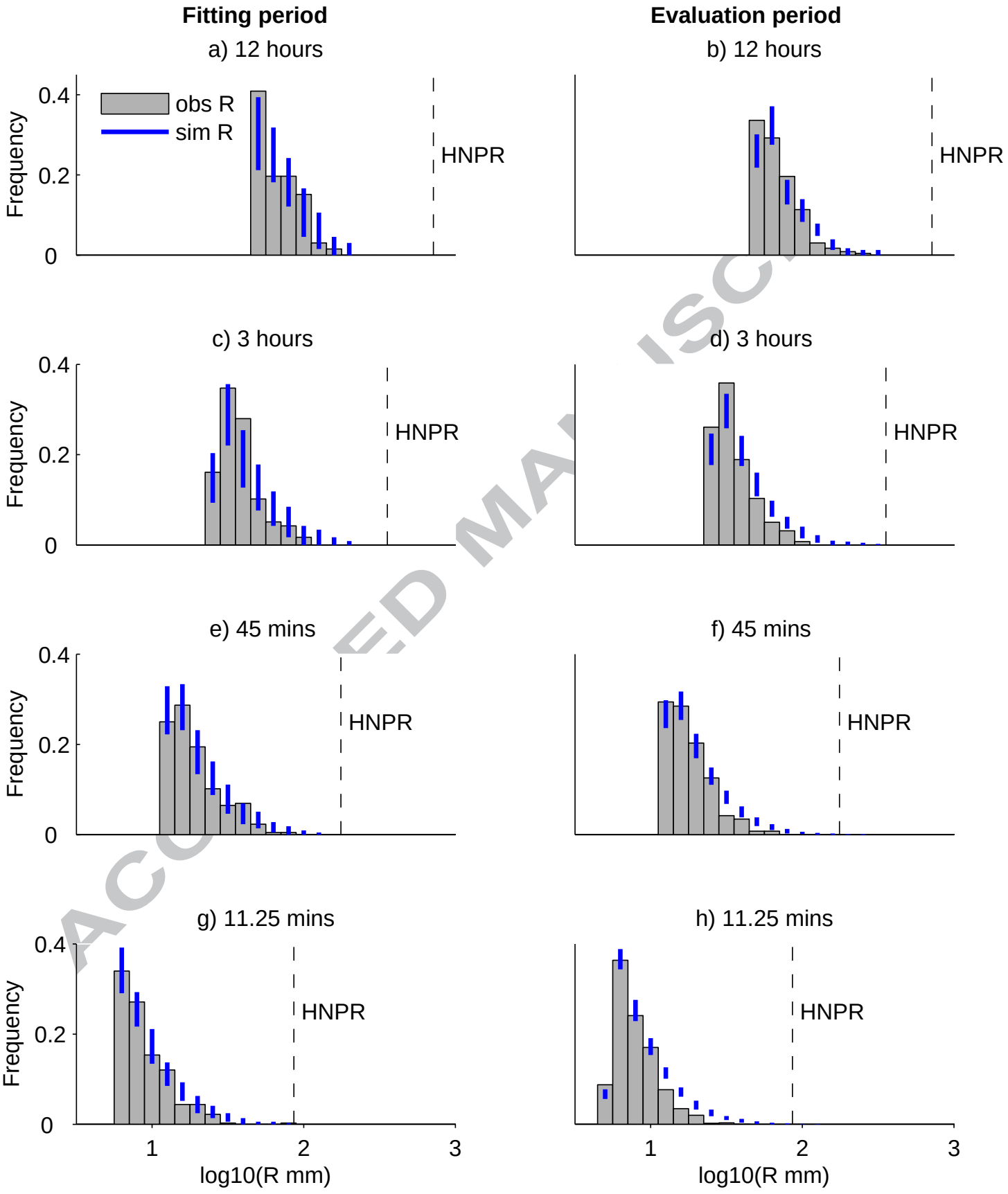

Figure A.2

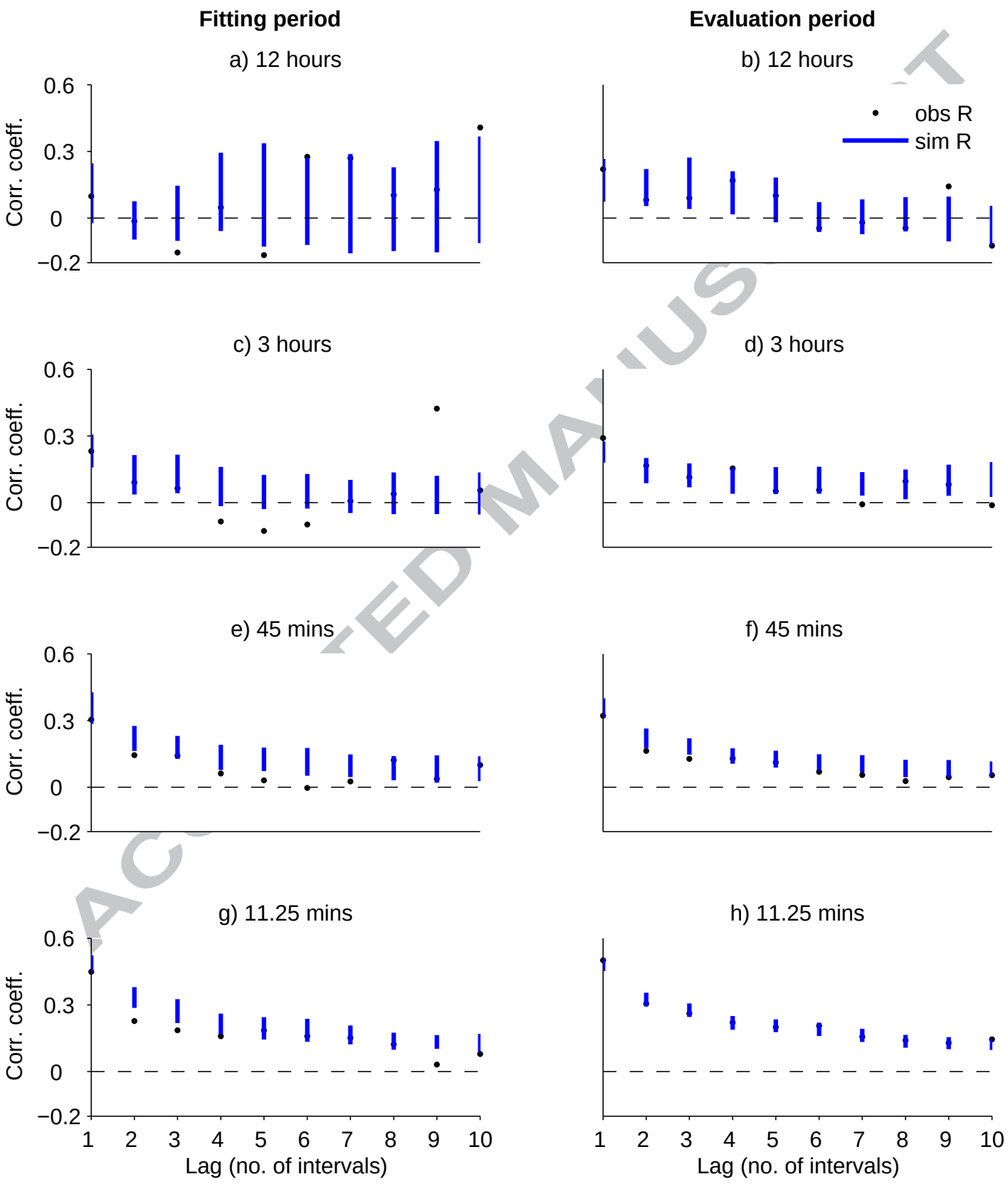

Highlights

- Volume of rainfall, time of day, season, structure of event have significant effects
- An analysis of 108 years of rainfall data show weak decadal scale trends
- A 16-parameter-per-level model performs well in terms of fine scale extremes
- Empirically derived scale dependence leads to a model with only 4 parameters
- The simple model almost matches performance of the original model